Improving the Performance of Photovoltaic Solar Panels Using Argon-Filled Double-Glazing Cover as a Radiative Cooling

Saddam K. Shabeeb[1*], Muna S. Kassim[1], Hussain H. Al-Kayiem[2]

[1] Mechanical Engineering Department, College of Engineering, Mustansiriyah University, Baghdad 10052, Iraq
[2] Air Conditioning and Refrigeration Techniques Engineering Department, Hilla University College, Babylon 51001, Iraq

Corresponding Author Email: saddam1975@uomustansiriyah.edu.iq

ABSTRACT

This study presents a new radiative cooling method to mitigate the radiation effect on a photovoltaic panel using a glass cover consisting of two glass panels. The gap between the perfectly sealed glass layers is filled with Argon gas as a heat suppressant. The assessment of the new proposed idea is performed experimentally and numerically. An experimental setup has been designed and fabricated to measure the required parameters for the system performance evaluation. The research parameters included design parameters such as the gap height between the glass layers at 10, 15, 20 and 25 mm. The tests were performed on various solar irradiances over the day. The output voltage, current, and temperatures at various locations were also recorded to permit performance evaluation. The investigations were extended by computational simulation to visualize the thermal situation at various design parameters. The results showed that there was a decrease in the panel surface temperature of the photovoltaic panels after adding the glass cover. By installation of the double glassing cover with a 20 mm gap, the surface temperature was reduced by between 5℃-9℃. Such temperature reduction demonstrates the success of the novel idea of an Argon-filled double-glassing cover. The maximum efficiency was increased to 14.2% for a panel with the added radiative cooler compared to 12.1% for a regular panel without cover under the same operating conditions.

1. INTRODUCTION

Among various solar energy conversion techniques for power generation, photovoltaics (PV) are mostly adopted in solar-to-electricity applications. However, PV cells still have some drawbacks due to the thermal effect and corresponding heat accumulation. The excess heat raises the temperature of the cell, causing a reduction in the conversion efficiency and degradation of the PV module components. Many cooling methods have been proposed and adopted, including water cooling, air cooling, integration with phase change materials in thermal energy storage, and selective and reflective coating, i.e., radiative cooling to mitigate the accumulated heat problem,

Photovoltaic cells receive about 80% of the incident solar radiation on their surface. Still, only 15-20 % of the incident radiation is converted to electric power depending on the electrical efficiency of the photovoltaic cells. The rest of the input solar energy is reflected in the ambient or accumulated as heat. The accumulated heat causes increasing in PV surface temperature [1], which may reach above its design temperature by more than 35℃ [2, 3]. Therefore, the biggest challenge that dilutes the performance of solar cells is caused by the high temperature [4], especially for first-generation PV modules [5]. The rise in the temperature of the cell negatively affects the

open circuit voltage of the photovoltaic cell [6], thus minimizing the output power. For crystalline silicon photovoltaic cells, it is found that the power efficiency decreases by 0.2%-0.5% for each 1.0°C rise in the temperature of the PV module above its design temperature, 25℃ [7, 8]. So, it is necessary to keep the temperature of the PV panel as low as possible.

In general, possible solutions to regulate the heat accumulated in the PV modules are based on cooling technologies, including air cooling, water cooling, PCM cooling, and special structure designs. Cooling strategies can be divided into two types: active cooling systems and passive cooling systems. An active cooling system requires an external energy source in the process of heat reduction using an electrical pump, fan, etc. A passive cooling system implements fixed components that mitigate the radiation or a natural source of cooling based on conduction or convection modes of heat transfer.

Radiative cooling becomes a matter of interest for PV productivity enhancement. It depends on the enhancement of heat emission, the absorption capacity of the cell, and the selectivity of the useful rays required for the solar units. Radiative cooling is the key factor that enables our planet (including buildings and objects) to satisfy a relatively constant temperature by emitting excessive heat to the

surroundings. The radiative cooling can be enhanced by increasing the emittance of the reflective surfaces. Thus, it is widely used as a method to cool and manage the heat for buildings, electronics, and solar panels [9]. Radiative cooling is based on the fact that the atmosphere transmits about 87% of the radiation coming out of the earth to the sky window region for a wavelength range of 8-13 μm [10]. Surfaces that emit strongly in this wavelength limit and reflect strongly outside this range witness an imbalance in outgoing and incoming thermal radiation and achieve a constant temperature lower than the ambient temperature [11].

Many studies have considered the passive radiative cooling method and spectral selectivity of the solar spectrum. Zhu et al. [12] designed a transparent coolant consisting of a two-dimensional square lattice of silica pyramids and a uniform silica layer of 100 μm thickness. This coolant is optically transparent and emits as a blackbody in the mid-infrared wavelength range. The results of performance predictions showed that even at a solar power of 800W/m², there is a temperature drop in the silicon solar cells with this design by 17.6℃, which subsequently leads to an improvement in the relative electrical efficiency by 7.9%. Zhu et al. [13] extended the work to include a transparent cooler manufactured by drilling grooves for air holes with a depth of 500 μm from a double-sided polished silica wafer. Spectral characterization showed that the grooved cooler has excellent heat emissivity in the infrared wavelength range and has high transmittance to the sun. The results have shown that the temperature of the silicon can be reduced by 14℃.

Wang et al. [14] have investigated the behavior of solar panels under concentrated radiation. They tested three categories of radiative cooling for limited heat and ambient conditions. The results revealed that the cooling methods may improve the performance by 25%-61% depending on the structure used. The obtained data explained the role of coupling cooling in decreasing the surface temperature of the panel by 35.9℃ for a limited source of heat. Hence, the voltage (V_{oc}) has been enhanced by 27%. Li et al. [15] adopted the idea of a full-spectrum thermal management system to cool solar cells. This method improved radiative cooling with a wide selective use of solar radiation. In the study, a commercial silicon solar cell was chosen as the primary device. The effective wavelength was measured to be 1.1 μm. Using materials such as silica, titanium dioxide, silicon nitride, and aluminum dioxide, a multilayer optical coolant was created. This coolant has a high transparency to effective photons and is highly reflective of undesired energy. In addition, the heat emission of the coolant was very high. The thermal simulation results indicated that the temperature of the solar panels can be decreased passively by more than 5.7℃ with the generated photonic coolant.

A coupled thermal-electrical modeling has been developed by Perrakis et al. [16] to study the mechanisms of how a radiative cooler affects the overall efficiency of commercial PV modules. The results indicated that it is possible to reduce the PV operating temperature by up to 10℃ (ideally) and achieve an increase in efficiency of up to 5.8% using a crystal PV structure that consists of alternating layers of thin films. The added alternating layers reduced the heat generation and reflected the sub-bandgap (Sub-BG), ultraviolet (UV), and infrared (IR) parts of the radiation band. Lu et al. [17] developed a passive cooling full-spectrum synergistic management technology for solar cells by deploying a spectral-selective mirror and a radiation cooler in the cell

cooling system to block sub-BG photons and enhance heat emission. Since the BG of a silicon cell is about 1.1eV, it should have a spectral-selective mirror with high reflectivity throughout the wavelength region 0.3-1.1 μm. This ensures that photons with energies greater than the BG may be reflected off the solar cells, which in turn generate electricity. In addition, the spectral-selective mirror must have low reflectivity in the wavelength region above 1.1 μm in order to block sub-BG photons as much as possible. For the suggested simulation conditions, the cell temperature has decreased by 7.1℃ and the open circuit voltage increased by 38mV.

Suryanto and Firman [18] have studied the vacuum technique for cooling PV cells. The research was carried out using an experimental method by conditioning the PV module under vacuum pressure (pressure < 1 bar). The PV cell has been put inside a translucent enclosure that offers a certain condition for the panel. The solar radiation can be passed easily through the glazed pane from the upper side. Results revealed that the vacuumed enclosure offered by the suggested case enabled the PV panel to improve its efficiency by 30% due to the reduction happened to the surface temperature of the panel from 45℃ to 30℃ for the cases without and with the enclosure, respectively.

Ahmadi Moghaddam et al. [19] have developed a CFD model to estimate the efficiency of a building-integrated photovoltaic (BIPV) system. Overheating of the panel was the main factor investigated by the study. Many parameters should be involved as well, such as the amount of radiation, the contribution of the convection, and the conduction of heat via the panel. The study assumed an emittance sheet upon the building surfaces and under the panel to play the role of radiative cooling. This mechanism offers a natural convection as well. The surface temperature of the PV panel has been reduced by 3℃, and the efficiency has improved by 21%.

From the previous works, it can be indicated that radiative cooling is very effective in reducing the undesired rays, thus decreasing the operating temperature of the solar cell by 6-36℃ and keeping its performance higher by 5-2%, depending on the conditions and applications. The literature shows that the optimum wavelengths for photoelectric conversion in solar cells range from 0.3-1.1 μm [20].

The parasitic absorption of wavelengths outside the optimum range causes a rise in the temperature of the photovoltaic cell, which leads to low photovoltaic conversion efficiency. This is due to the large drop in the open circuit voltage (V_{OC}) and the marginal rise in the short circuit current (I_{SC}) [21]. The open circuit voltage is directly proportional to the amount of light that enters the cell. It is strongly affected when the temperature of the cell or unit increases. The resistance of the circuit also increases with the increase in temperature due to the increase in the speed of the electrons. Other factors that affect the performance of a photovoltaic system are humidity, wind speed, shading, orientation of the panel, and accumulated dust (Agyekum et al. [22]).

Excessive heat accumulated in the solar PV panels due to high irradiance reduces the performance of the PV. Then, heat dissipation is essential to maintain the level of PV production performance and maximize electric power generation. Previous approaches for mitigating the excessive heat in a PV panel are passive and active water, air, and PCM cooling, i.e., PV/T approaches. The state-of-the-art is the radiative cooling techniques.

The main objective of this research is to introduce and assess the effectiveness of a novel radiative cooling approach

using an Argon-filled double-glazing unit situated on the upper surface of the PV panel. The propped approach has been investigated experimentally and numerically at various gap heights and operational solar irradiance. The computational simulations further assisted in understanding the thermal distribution in the PV module at various design and solar conditions.

2. MATERIALS AND METHODS

The main idea of the current research is to evaluate a new radiative cooling by a glazing unit consisting of two glazed panes separated by an Argon filled gap. The glass-Argon-glass (G-Ar-G) system works as a mitigating unit for the incident radiation or as a filter to reduce the undesired rays that cause the overheating of the PV module. The operational strategy of the proposed radiative cooling unit is presented in Figure 1.

The evaluation of the proposed Argon-filled double-glazing to reduce the PV temperature by radiative cooling and enhance the PC panel performance is performed experimentally and computationally.
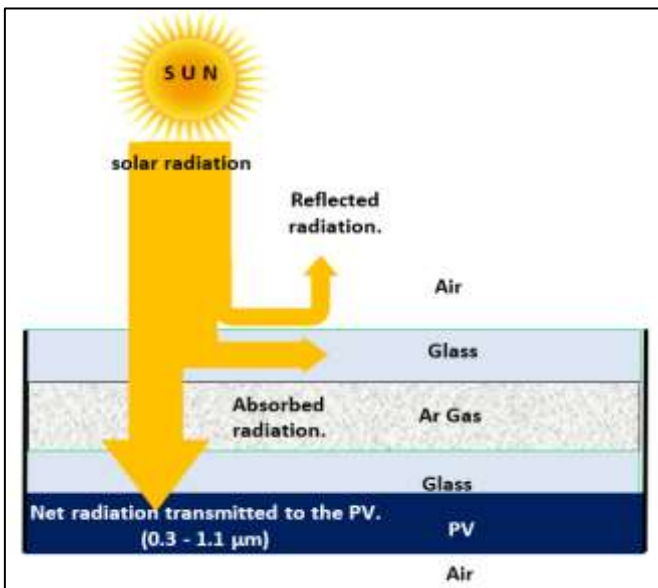

Figure 1. Schematic diagram of the glazing unit adopted in the experimental measurements

2.1 Experimental methodology

In this section, the development of the proposed radiative cooling unit, the design and construction of the experimental setup, and the experimental measurement procedure are detailed and discussed.

2.1.1 Development of the Argon-filled double-glazing unit
The proposed radiative cooling unit was constructed from two 4-mm-thick glass sheets with a perfectly sealed gap between them. Four units have been constructed with different gap thicknesses, as shown in Figure 2. The selected gaps for the current investigations are 10, 15, 20, and 25 mm. Accordingly, four units have been fabricated. Two valves are installed for filling and emptying the Argon in the space between the glass layers. The surface area of the unit is 500 mm wide and 670 mm long.


(a)

(b)
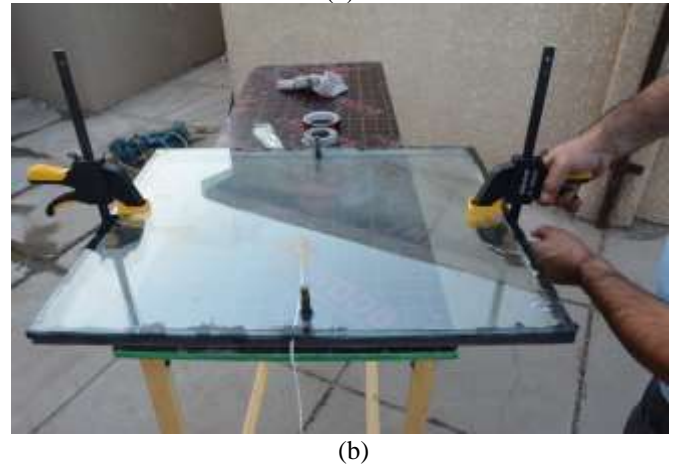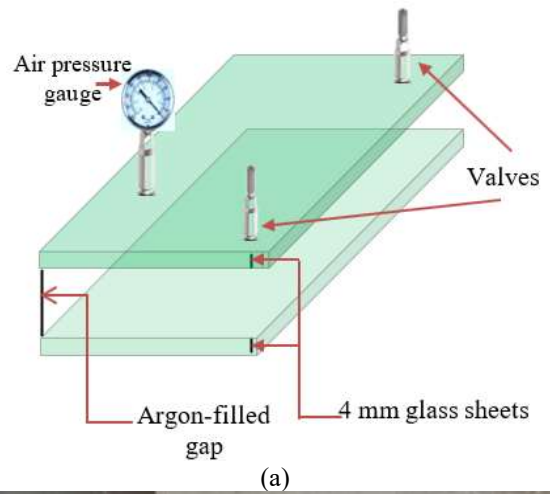
Figure 2. (a) Schematic of the Argon-filled double-glazing unit, and (b) Physical photo of the Argon-filled double-glazing unit for radiative cooling

2.1.2 Construction of the experimental setup
The experimental setup consists mainly of two PV panels and a set of measuring instrumentations, as shown in Figure 3. One is the bare PV used as a reference, and the radiative cooling unit covers the second. Having two units allows simultaneous measurements for proper comparison of the system performance and highlights the enhancement caused by the radiative cooling, properly. The PV panel used was an FRS-50W multi-crystalline solar cell with specific features shown in Table 1. The experimental setup was placed on the terrace floor of a typical building in Baghdad. The panels have been orientated toward the south and tilted by 30o as an optimum choice, as recommended by Al-Shohani et al. [5]. The experimental setup is equipped with several instruments to record the experimental variables. The temperatures of the surfaces have been measured in four Type-K thermocouples connected to a data logger (Reed-947SD). A solar power meter (SM-206) has been used to measure the solar irradiation. A solar panel multimeter has been used to measure the voltage and current of the PV panel.

The research program lasted for around five months, from May - September 2023. The measurements have been recorded on an hourly base and repeated for many days to reduce the uncertainty of results, where the mean of the multi-days is considered. Each experiment started at 08:00 AM and ended at 04:00 AM. The entire operational conditions related to the current study are shown in Table 2.
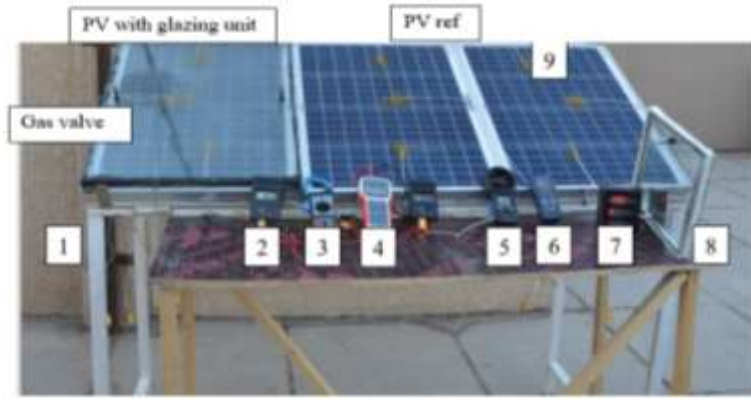
Figure 3. The experimental setup consisted of a bare PV panel and modified PV with an Argon-filled double-glazing unit with the measuring instruments

Note: 1: Structure; 2: Data logger; 3: Electrical reader; 4: Solar panel multimeter; 5: Anemometer; 6: Solar meter; 7: Optical transmittance meter; 8: Double glazing unit; 9: Thermocouple

Table 1. Specification of the photovoltaic panel used in the current study

Item	Features
Module type	FRS-50W
Peak power (PMax)	50W
Maximum power voltage (VMP)	18V
Maximum power current (IMP)	2.78A
Short circuit current (I_{SC})	2.97A
Open voltage (V_{OC})	22.05V
Tolerance	±3%
Application class	A
Fuse rating	15A
Dimensions	50×67×3.5cm^3
Standard test condition (STC)	AM1.5, 25°C, 1000W/m^2

Table 2. Operational conditions for the current study

Item	Value or Description
PV modules	Two PV panels: 1. Without glazing cover, bare case. 2. With double-glassing Argon-filled cover.
Dimensions of each PV panel	500-mm-wide, 670-mm-long, 35-mm-thick
Features of a glazing unit	Argon-filled double-glazing
Gas gap thickness	10, 15, 20, and 25 mm
Ambient temperature conditions	Summer, Max. Temperatures on the experiment days are 35-50°C
Solar conditions	The lowest peak is 750W/m^2 and max. peak 1080W/m^2
Location	On the terrace floor of a typical building in Baghdad

2.2 Computational method

2.2.1 Computational model

The numerical investigation has been carried out using ANSYS FLUENT commercial software. The specifications and physical properties of both the PV module and the suggested Argon-filled double-glazing unit are specified and modeled, as shown in Figure 4. The specifications of the PV module and the physical properties used in the computational simulation are shown in Table 3. The specification of the Argon-filled double-glazing unit, and the physical properties are shown in Table 4.

**Table 3.** Specifications of photovoltaic unit [23]

Material	Thickness (mm)	Density (kg/m^3)	K (W/ m·K)	C$_p$ (J/kg·K)	Absorptivity λ	Reflectivity σ	Transmissivity τ	Emissivity ε
Glass	3.0	3000	2.0	500	0.04	0.04	0.92	0.9
EVA	0.5	960	0.35	2070	0.08	0.02	0.9	-
Solar cell	0.3	2330	148	677	0.9	0.08	0.02	-
Tedlar	0.1	1200	0.2	1250	0.13	0.86	0.012	0.9

Table 4. Specifications of double-glazing system [24]

| Material	Thickness (mm)	Density [kg/m^3]	Thermal Conductivity [W/ m·K]	C$_p$ [J/kg·K]	Absorptivity λ	Reflectivity σ	Transmissivity τ	Emissivity ε
Glass	4	3000	2.0	450	0.4	0.03	0.93	0.9
Ar gas	10-25	1.78	0.018	520.3	0.67	0.04	0.29	-

2.2.2 Generation of the computational models

The 3D model was represented in ANSYS software, where the PV panel consists of five layers, as shown in Figure 4(a). Two layers of glass were placed above the PV upper surface. The gap between the double-glazing sheets was filled with Argon, as shown in Figure 4(b).
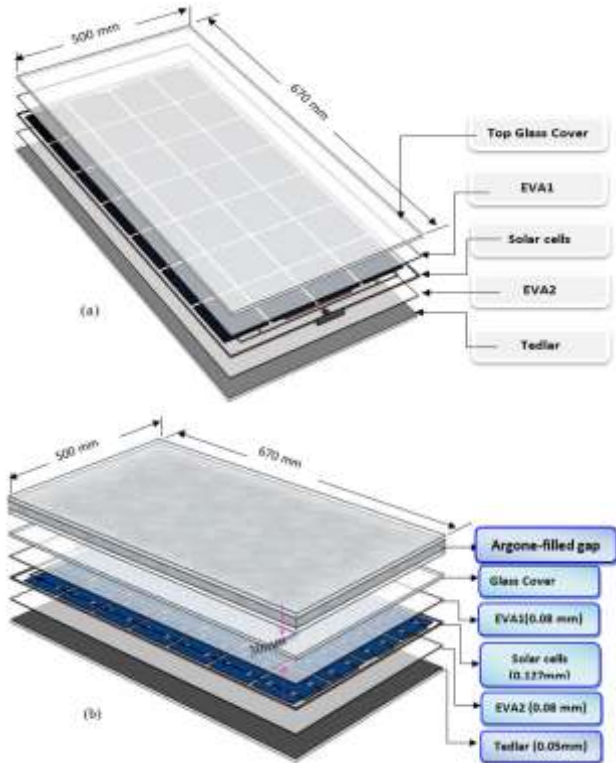
Figure 4. (a) Geometries of PV standard model; (b) Geometries of modified PV with double glazing (DG-gas) model

2.2.3 Mesh generation
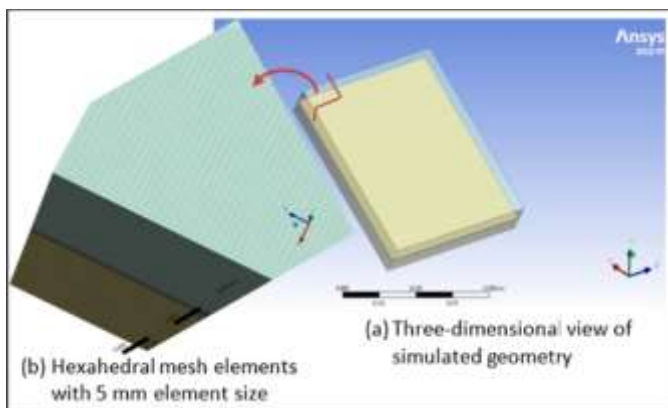
Figure 5. Geometry and mesh of the computational model

The mesh generation is the most essential step in ANSYS FLUENT model creation. There are three types of mesh in common: structured, unstructured meshing, and the combination of them. Structured mesh elements can be hexahedral, while unstructured mesh elements can be tetrahedral, prismatic, or pyramidal. In order to check for the best mesh generation, an analysis of network independence is performed on the PV system covered by an Argon-filled double-glazing unit. As depicted in Figure 5, the simulation

results of the system are compared for various degrees of network accuracy. It can be seen that the hexahedral network with a 5 mm element size yields the most acceptable results with no significant variation in accuracy.

In contrast, the time required for network generation and analysis is nearly cut in half when compared to the case of tetrahedral elements. This is because the geometry is straightforward, and it is always advised to use a hexahedral grid when the geometry is straightforward (Tadepalli et al. [25]). In total, the suggested mesh has 4640413 nodes and 442368 elements.

2.2.4 Boundary conditions and governing equations

Choosing the relevant set of environmental conditions is important to evaluate the potential of a cooling strategy. In fact, the expected temperature drop attributed to radiative cooling varies greatly depending on the level of solar and atmospheric radiation, ambient temperature, and wind speed. Defining reference climatic conditions is also essential to compare capabilities between technologies. To demonstrate the potential in terms of temperature reduction and power enhancement, we need these conditions to be conducive to radiative cooling while remaining close to real operating conditions.

For proper thermal modelling, the following assumptions are taken into account.

- The temperature of the different layers of the PV module remains the same everywhere.
- It is assumed that their thermophysical properties do not change with changes in temperature.
- It is assumed that ohmic losses in photovoltaic cells are negligible.
- The boundary conditions applied to this study are assumed to be.
- Based on commercial PV module.
- The sidewalls are opaque as the aluminium frame covers the sidewalls of most commercial PV modules.
- The sides of the gas filter are opaque due to the adhesive present between the upper and lower layers of glass.
- The effect of convective heat transfer is not taken into account for all PV cell walls.
- The calculated radiative heat flux is introduced as the boundary energy source into the energy equation.
- The mesh is created using a quad mesh type.

2.2.5 Governing equations

Navier-Stokes equation is introduced to describe the airflow field and thermal behaviour of the PV module. The differential equations governing heat transfer, including conservation of mass, momentum, and energy, are presented. Local thermal equilibrium was used to model the thermal field around the PV module. All equations are displayed in Cartesian coordinates.

- Conservation of mass:

The mass change within a control volume must equal the sum of the mass inflow and outflow through the control volume surface. This can be mathematically expressed as follows for an incompressible fluid:

$$\frac{\partial u}{\partial x} + \frac{\partial v}{\partial y} + \frac{\partial w}{\partial z} = 0 \qquad (1)$$

where u, v, and w are the three components of velocity corresponding to the x, y, and z directions, respectively.

- Momentum equations in x, y, and z directions:

$$\rho_f \left[u\frac{\partial u}{\partial x} + v\frac{\partial u}{\partial y} + w\frac{\partial u}{\partial z} \right]$$
$$= -\frac{\partial \rho}{\partial x} + \mu_f \left[\frac{\partial^2 u}{\partial x^2} + \frac{\partial^2 u}{\partial y^2} + \frac{\partial^2 u}{\partial z^2} \right] \qquad (2)$$

$$\rho_f \left[u\frac{\partial v}{\partial x} + v\frac{\partial v}{\partial y} + w\frac{\partial v}{\partial z} \right]$$
$$= -\frac{\partial \rho}{\partial x} + \mu_f \left[\frac{\partial^2 v}{\partial x^2} + \frac{\partial^2 v}{\partial y^2} + \frac{\partial^2 v}{\partial z^2} \right] \qquad (3)$$

$$\rho_f \left[u\frac{\partial w}{\partial x} + v\frac{\partial w}{\partial y} + w\frac{\partial w}{\partial z} \right]$$
$$= -\frac{\partial \rho}{\partial x} + \mu_f \left[\frac{\partial^2 w}{\partial x^2} + \frac{\partial^2 w}{\partial y^2} + \frac{\partial^2 w}{\partial z^2} \right] \qquad (4)$$

- Energy equation

The energy equation for the fluid and solid domains is:

$$C_{pf} \rho_f \left[u\frac{\partial T}{\partial x} + v\frac{\partial T}{\partial y} + w\frac{\partial T}{\partial z} \right]$$
$$= k_f \left[\frac{\partial^2 T}{\partial x^2} + \frac{\partial^2 T}{\partial y^2} + \frac{\partial^2 T}{\partial z^2} \right] \qquad (5)$$

- Short circuit current (I_{SC}) and Open circuit voltage, V_{OC}, Shen et al. [26]:

$$I_{sc} = I_{ref}[1 + \alpha_{ref}(T_{sc} - T_{ref})] \qquad (6)$$

$$V_{oc} = V_{ref}[1 - \beta_{ref}(T_{sc} - T_{ref})] \qquad (7)$$

$$P_{max} = P_{ref}[1 - \gamma_{ref}(T_{sc} - T_{ref})] \qquad (8)$$

where the subscript, "$_{ref}$" represents the condition at a temperature of 25°C, which is the optimum operating temperature of PV modules at the rated power. T_{SC} is the solar cell operating temperature. I_{SC} is the short circuit current. V_{OC} is the open voltage. Pmax is the peak power. The symbols α, β and γ denote the coefficients assigned for the variation with temperature for current, voltage, and power, respectively.

The fill factor (FF) displays the maximum power output that can be achieved. The following equation can express this factor, Smets et al. [27]:

$$FF = \frac{P_{max}}{V_{oc}\, I_{sc}} \qquad (9)$$

The solar efficiency of a photovoltaic panel, η_{sc} can be defined as the ratio of electrical energy output to incident radiation and could be expressed as [27]:

$$\eta_{sc} = \frac{P_{max}}{G\,A} = \frac{I_{sc} * V_{oc}}{G\,A} \qquad (10)$$

In terms of temperature, as follows [28]:

$$\eta_{sc} = \eta_{ref}(1 - \beta_{ref}(T_{sc} - T_{ref})) \qquad (11)$$

where,
η_{ref} is the reference efficiency of the PV module ($\eta_{ref} = 0.12$).
β_{ref} is the temperature coefficient ($\beta_{ref} = 0.0045°C^{-1}$).
T_{sc} is the solar cell temperature.
T_{ref} is the reference temperature (25°C).

3. RESULTS AND DISCUSSION

This section discusses the verification of the experimental measurement procedure, the validation of the computational procedure, and the experimental and numerical results. Most of the experimental results have been presented in graphical format to point out the effectiveness of the added double glassing with different gap thicknesses that are filled with Argon. The CFD results are mostly presented as temperature contours.

3.1 Analysis of experimental results

The experimental results consisted of verification, testing conditions, and experimental measurement analysis.

3.1.1 Verification of the experimental procedure

The experimental procedure has been verified by comparison with previous experimental results reported by Jaffar et al. [29], as shown in Figure 6. The results of the current study agree satisfactorily with the experimental measurements of the study [29]. The mean relative percentage of difference is 7.5%. In terms of trend, both experimental works show the same trend of transient temperature increase in the morning and gradually after 11:00 AM. The comparison of results demonstrates the verified experimental procedure of the current work.

The main reason for the small difference of 7.5% is the weather data, as Jaffer et al. conducted the measurement in July. The average solar irradiance was recorded at a maximum value of about 980W/m² at 12:00 PM, and the maximum average ambient temperature was 48°C. In contrast, the current experimental measurement that is compared to Jaffer et al. was performed in May with a maximum solar irradiance of 720W/m² and ambient temperature of 38°C.
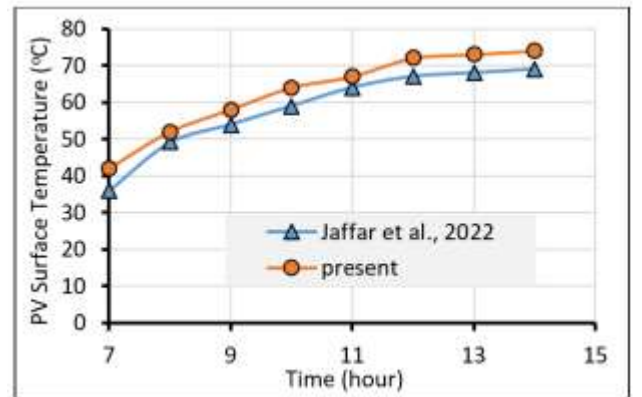

Figure 6. Verification of the experimental procedure by comparison with measurement data reported by Jaffar et al. [29]

3.1.2 Experiment environment conditions

The recorded ambient temperature and solar irradiation during the measurement period are shown in Figure 7. The

maximum ambient temperature is 32°C in May and 49°C in August. The maximum temperature is usually recorded between 1-2 PM. On the other hand, the solar radiation ranged between 750W/m² in May to 1080W/m² in July. The maximum irradiation is usually recorded around 12:00 to 01:00 PM.
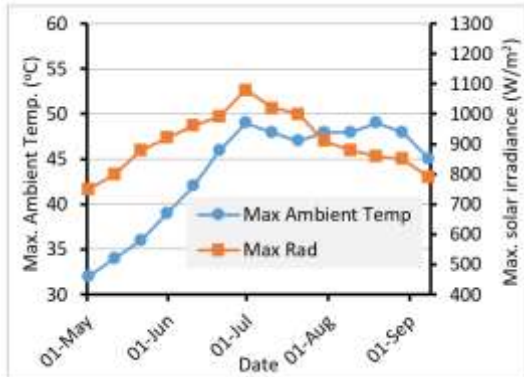
Figure 7. Recorded values for ambient temperature and radiation during the summer

3.1.3 The effect of the cover unit on the PV temperature

The installed cover unit has a direct effect on the surface temperature of the solar panel. This is mostly due to the attenuation of the incident radiation, where the photons responsible for the overheating, especially when the rays are outside the optimum range of the solar spectrum (0.3-1.1 μm). The more solar radiation outside the mentioned range, by reflection, the faster the panel temperature will drop.

The reason behind the reduction of temperature is attributed to the glazing unit in mitigating all modes of heat transfer: conduction, convection, and radiation. When the incident radiation lies on the external pane, heat can move directly through the glass via conduction. However, the light that passes through the glass gets reflection and refraction as well. Additionally, as light moves from the air into the dense glass, it slows down Liu [30]. In a double-glazing system, the movement of gas within the gap can also contribute to heat transfer via convection. Warm gas near the inner face of the external pane may circulate to the internal pane via natural or free convection. Also, the Argon in the gap reduces both conduction and convection. Argon has a lower thermal conductivity than air (Cuce [31]), so it inhibits heat transfer by conduction. Additionally, Argon is denser than air (Sismanoglu et al. [32]), which means a reduction in the natural movement of gas and minimizes heat transfer through convection.

The results, shown in Figure 8, represent the PV surface temperatures of the panel during daytime hours (8:00 AM-5:00 PM) without and with coverage by the Argon-filled double-glazing unit. The surface temperature that was measured experimentally reached its maximum value around 1:00 PM. Initially, the maximum temperature of the PV panel without the glazing unit (GU) was 65.9°C. By incorporating the glazing unit with a gas thickness of 10 mm, the temperature of the PV panel has decreased to 60.4°C, i.e., the difference is 5.5°C, as shown in Figure 8(a). When the thickness of the gas space was 15 mm, the PV maximum temperature was decreased to 59.1°C, i.e., the difference was 6.0°C, as shown in Figure 8(b).

Moreover, with a 20 mm thickness, the maximum temperature of the PV panel has decreased to 56.7°C, as shown
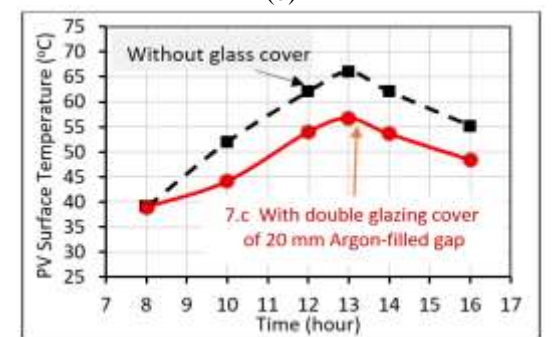
in Figure 8(c). This represents the optimum case, where the difference in maximum surface temperature is 9.2°C compared to the bare case. By further increasing the Argon gap thickness to 25 mm, the maximum temperature of the PV panel decreased to 58.8°C, i.e., the difference is 7.1°C, as shown in Figure 8(d).
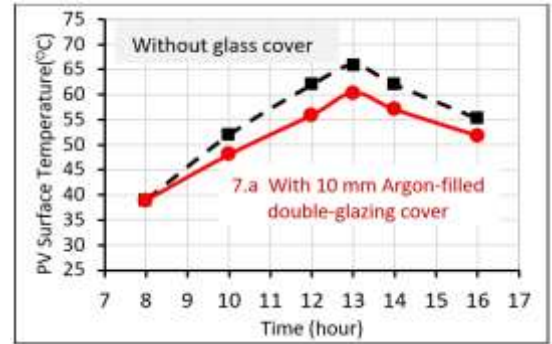

(a)

(b)

(c)

(d)

Figure 8. (a) Surface temperature of the PV panel with and without the glazing unit (10 mm); (b) Surface temperature of the PV panel with and without the glazing unit (15 mm); (c) Surface temperature of the PV panel with and without the glazing unit (20 mm); (d) Surface temperature of the PV panel with and without the glazing unit (25 mm)

**3.1.4 The effect of the glazing unit on the performance of the PV panel**

The performance of using the glazing unit has been evaluated by measuring the variation happened to the current, the voltage, and the fill factor (FF) for different gas gap thicknesses. The characteristics of open circuit voltage, V_{OC}, short circuit current (I_{SC}), and maximum power, Pmax, can be represented for a typical solar cell with respect to the solar cell temperature, T_{sc}, according to the Eqs. (6)-(8).

The short circuit current is highly dependent on light intensity; therefore, the most sensitive parameter of the solar cell to the temperature variation is the voltage [33]. The I-V curves are shown in Figure 9 for different cases. The current is mostly constant at 3A for a wide range of the working voltage. The values of the voltages have shown improvement by increasing the thickness of the gas space. Initially, without a glazing unit, the maximum current was 3.0A, and the maximum voltage was 18.0V. The voltage increases in the presence of the glazing unit to be 19.5, 21.8, 24.1 and 22.4V at a thickness of the gas space of 10, 15, 20, and 25 mm, respectively. The optimum increasing in the voltage was 24% for the case of 20 mm. Since the cell efficiency relates directly to the voltage, the increase in the voltage enhances the cell efficiency.
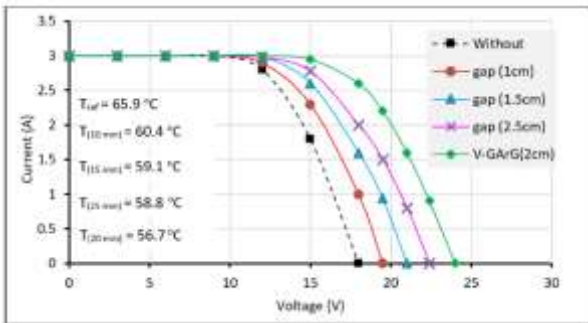

Figure 9. Variation of the voltage with different thicknesses of the glazing unit

The fill factor displays the maximum power output that can be extracted from the short circuit current to the open circuit voltage at the maximum power. Thus, this factor can be expressed by Eq. (9). Figure 10 shows the variation of FF with the thickness of the gas space. The maximum FF was 76.3% when the glazing unit was present with a gap of 20 mm, while the maximum FF in the absence of the glazing unit was 73%.
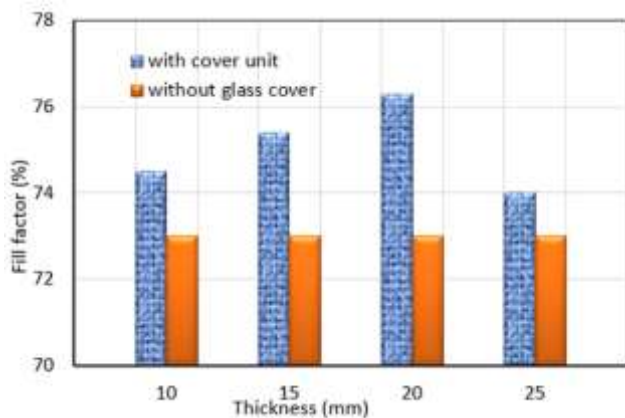
Figure 10. Variation of the fill factor with different thicknesses of the glazing unit (on 15 August 2023)

The solar-to-electricity conversion efficiency of the system has been calculated in the daytime period for the conditions with and without a glazing unit, as shown in Figure 11. In general, there is an enhancement in the overall efficiency when the Argon-filled double-glazing unit covers the PV. It is 8% higher at the peak time when the Argon gap is 20 mm. The system with a glazing unit showed a mean daily efficiency of 14.9%, which is higher than the case without a glazing unit, 12.8%. Hence, the PV system showed an improvement in efficiency by 13.7% for the same operating conditions.
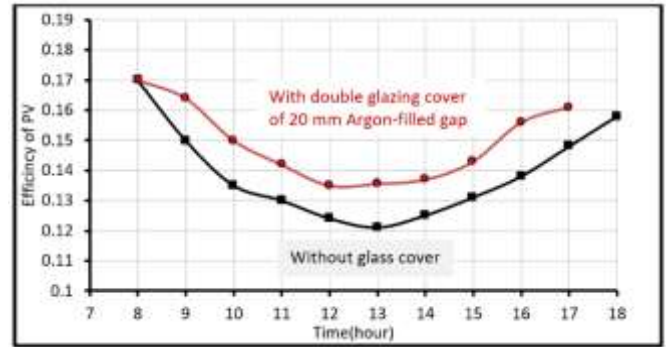

Figure 11. Variation of the efficiency with time for the PV panel, with and without GU (on 15 August 2023)

3.2 Numerical results

3.2.1 Validation of the computational procedure

To prove the correctness of the numerical results, both geometric and parametric conditions were used quite similar to the experimental test rig. The measured and predicted PV surface temperatures are compared, as shown in Figure 12. Comparison results show a satisfactory convergence between the numerical simulation and the experimental experimental measurement results. Maximum discrepancies between numerical and experimental results were 10.4%, 11.8%, 13.1%, and 9.7% for the cases 10, 15, 20, and 25 mm, respectively. The trends of all cases are similar as the PV temperature increases and reaches the peak around 01:00 PM, and then reduces till the end of the measurement period. The experimental results of the PV temperature are slightly higher than the simulation prediction. The reasons for the difference between the experimental and the numerical results are due to the measuring devices used and the accuracy of some material properties assumed in the simulation. However, there is a satisfactory convergence between the results obtained from the computational simulation and the experimental measurements.
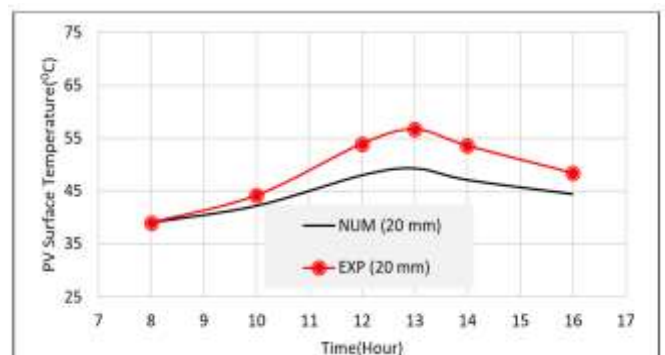
Figure 12. Comparison between the experimental and the numerical results for the case of 20 mm Argon-filled double glassing

3.2.2 Temperature distribution over the PV panel
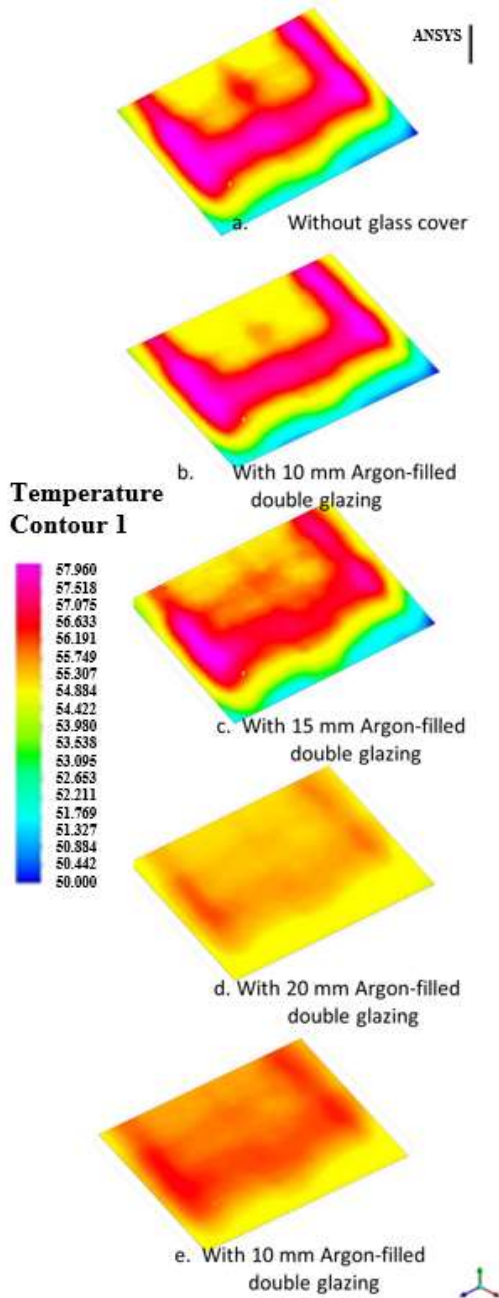
Figure 13. The temperature distribution over the upper surface of the PV panel

Figure 13 shows the distribution of temperatures over the entire PV panel extracted from the numerical simulation. The figures are assigned for different thicknesses of Argon-filled gaps ranging between 10-25 mm at 01:00 PM on 25 August 2023. The panel without the glazing unit appeared mostly at extremely high temperatures at the peak time between 62℃ to 65℃. By the installation of the Argon-filled double-glazing unit, the range of PV temperatures was reduced to 50℃-58℃, 47℃-55℃, 45℃-53℃, and 49℃-56℃ for 10, 15, 20, and 25mm Argon gap thickness, respectively. The optimum decrease appeared when the Argon gap thickness was 20 mm, where the mean PV module surface temperature was around 48℃. The experimental results showed a 9.2℃ PV maximum temperature reduction in the case of 20 mm Argon gap thickness, while the numerical results showed a reduction of around 11℃.

3.3 Comparison with previous techniques

Table 5. Comparison of the PV cooling techniques

Radiative Technique	Author(s)	Remarks
Glass cover Single 3 mm	Sato and Yamada [34]	The emissivity spectrum of a PV module surface hardly contributes to the enhancement of the radiative cooling performance for wide-ranged climate conditions. The reduction is ~ 1℃.
Glass cover Single 3.2 mm	Zhao et al. [35]	1.0℃ lower than that in the commercial structure.
Glass cover Single 3.2 mm coated with a polydimethylsiloxane film	Zhao et al. [35]	PV temperature could only be reduced by 1.75 K, even in the ideal case.
Selective coating by silica, titanium dioxide, silicon nitride, and aluminum dioxide	Li et al. [15]	Experimental and simulation results show no specific potential for cooling solar cells. High transparency to effective photons and is highly reflective of undesired energy. Results indicated that the temperature of the solar panels could be decreased passively by more than 5.7℃.
PV cooler consisting of a two-dimensional square lattice of silica pyramids	Zhu et al. [12]	Experimental and simulation showed that the temperature of the silicon solar cell decreased by 17.6℃ at 800W/m² irradiation.
Transparent cooler with grooves for air holes with a depth of 500 μm from a double-sided polished silica wafer	Zhu et al. [13]	14℃ could reduce the temperature of the silicon PV.
PV is covered by double glassing with a gap filled with Argon and has 10, 15, 20 and 25 mm height.	Current work	PV maximum temperature reduced by: 5.5℃ with a gas gap of 10 mm 6.0℃ with a gas gap of 15 mm 9.2℃ with a gas gap of 15 mm 7.1℃ with a gas gap of 15 mm Overall efficiency improvement of 12%

Dwivedi et al. [36], in their review papers, and Al-Waeli et al. [37], in their book, have covered a wide range of PV cooling technologies. It could be concluded from the presentation in the studies [36, 37] that PV cooling is known to be either active or passive, using fluid, nanofluids, and PCM as mediums for heat dissipation. However, the new trend, which is adopted in the current study, is radiative cooling, also named photonic cooling, which is categorized under the

passive cooling technique.

Active cooling requires a coolant, like air or water, which typically involves fan or pump power, whereas passive cooling requires no special power to cool PV cells [38, 39]. Passive cooling might include extra components, like heat pipe or sink or exchanger to drive natural convection cooling [40]. Radiative cooling, like passive cooling, does not require circulation. Passive cooling technologies are, therefore, considered to be effective in reducing the temperature of PV cells, as they are relatively easy and cost-effective to produce. Radiative cooling has been reviewed by Sato and Yamada [34], and some comparative data were presented.

Radiative cooling may be achieved by glass coverage of the PV or surface modification to manage the absorbed, transmitted, and reflected wavelength. The current study adopted radiative cooling with a new reflective technique by Argon filled double glassing cover. The new verified approach is compared to other radiative techniques, as shown in Table 5.

The most effective PV radiative cooling technique is surface modification to limit the spectrum of solar radiation that penetrates through the upper surface. However, the production technology is a challenge. Also, the cleaning of the accumulated dust is a major setback in the surface modification. In contrast, the Argon-filled double-glazing cover is easy to manufacture, low cost, and easy to clean. Further investigations with other gases and various gap heights may demonstrate more temperature reduction that may make it competitive to the surface modification radiative cooling.

4. CONCLUSION

An Argon-filled double-glazing coverage unit is suggested and investigated experimentally with various Argon gap thicknesses to assess its effect on enhancing the performance of PV modules by reducing the temperature by radiative cooling. The newly introduced radiative cooling unit is tested with Argon gaps of 10, 15, 20 and 25 mm thicknesses. Results show that the suggested unit is capable of reducing the PV panel surface temperature, thus enhancing its performance during extreme hot conditions. This thickness allows transmission of the solar spectrum within acceptable wavelengths and reflects or dissipates the remaining. With its optimum conditions, the proposed Argon-filled double-glazing reduced the temperature of the PV panel by 5℃-9.2℃, improved the voltage by 24%, and increased the fill factor from 73% for the case without glazing to 76.3% with a 20 mm Argon gap. The system efficiency is improved by 12% compared to the PV panel without cover. The optimum thickness of the Argon gap is 20 mm,

It is recommended to investigate the idea of the Argon-filled double-glazing radiative cooling with another type of gas. Air is recommended to be tested with various air gap thicknesses. In addition, a feasibility study of using the newly introduced technique of radiative cooling is recommended to be estimated and compared with other PV cooling techniques, counting for the costs of materials, maintenance, payback years, and production LCOE.

ACKNOWLEDGMENT

REFERENCES

[1] Rasool, I.N., Abdullah, R.S. (2023). Experimental study of PV panel performance using backside water cooling chamber. International Journal of Energy Production and Management, 8(2): 89-95. https://doi.org/10.18280/ijepm.080205

[2] Radziemska, E. (2003). The effect of temperature on the power drop in crystalline solar cells. Renewable Energy, 28: 1-12. https://doi.org/10.1016/S0960-1481(02)00015-0

[3] Xu, Z., Kong, Q., Qu, H., Wang, C. (2023). Cooling characteristics of solar photovoltaic panels based on phase change materials. Case Studies in Thermal Engineering, 41: 102667. https://doi.org/10.1016/j.csite.2022.102667

[4] Al-Kayiem, H.H., Reda, M.N. (2021). Analysis of solar photovoltaic panel integrated with ground heat exchanger for thermal management. International Journal of Energy Production and Management, 6(1): 17-31. https://doi.org/10.2495/EQ-V6-N1-17-31

[5] Al-Shohani, W.A.M., Khaleel, A.J., Dakkama, H.J., Ahmed, A.Q. (2022). Optimum tilt angle of the photovoltaic modules in Baghdad, Iraq. Applied Solar Energy, 58(4): 517–525. https://doi.org/10.3103/S0003701X22040028

[6] Chehreh, S.S.C. (2021). An enviroeconomic review of the solar PV cells cooling technology effect on the CO2 emission reduction. Solar Energy, 216: 468-492. https://doi.org/10.1016/j.solener.2021.01.016

[7] Mohammed, F.M., Mohammed, J.A.K., Sanad, M.A.S. (2019). Performance enhancement of photovoltaic panel using double-sides water glazing chambers cooling technique. Al-Nahrain Journal for Engineering Sciences, 22(1): 22-30.

[8] Parthiban, R., Ponnambalam, P. (2022). An enhancement of the solar panel efficiency: A comprehensive review. Frontiers in Energy Research, 10: 937155. https://doi.org/10.3389/fenrg.2022.937155

[9] Zhu, L., Raman, A., Fan, S. (2013). Color-preserving daytime radiative cooling. Applied Physics Letters, 103(22). https://doi.org/10.1063/1.4835995

[10] Hossain, M.M., Jia, B., Gu, M. (2015). A metamaterial emitter for highly efficient radiative cooling. Advanced Optical Materials, 3(8): 1047-1051. https://doi.org/10.1002/adom.201500119

[11] Aili, A., Zhao, D., Lu, J., Zhai, Y., Yin, X., Tan, G., Yang, R. (2019). A kW-scale, 24-hour continuously operational, radiative sky cooling system: Experimental demonstration and predictive modeling. Energy Conversion and Management, 186: 586-596. https://doi.org/10.1016/j.enconman.2019.03.006

[12] Zhu, L., Raman, A., Wang, K.X., Anoma, M.A.,Fan, S. (2015). Radiative cooling for solar cells. Physics, Simulation, and Photonic Engineering of Photovoltaic Devices IV, 9358: 935814. https://doi.org/10.1117/12.2080148

[13] Zhu, L., Raman, A.P., Fan, S. (2015). Radiative cooling of solar absorbers using a visibly transparent photonic crystal thermal blackbody. Proceedings of the National

Academy of Sciences of the United States of America, 112(40): 12282-12287. https://doi.org/10.1073/pnas.1509453112

[14] Wang, Z., Kortge, D., Zhu, J., Zhou, Z., Torsina, H., Lee, C., Bermel, P., Wang, Z., Kortge, D., Zhu, J., Zhou, Z., Torsina, H., Lee, C. (2020). Lightweight, passive radiative cooling to enhance concentrating photovoltaics lightweight, passive radiative cooling to enhance concentrating photovoltaics. Joule, 4(12): 2702-2717. https://doi.org/10.1016/j.joule.2020.10.004

[15] Li, W., Shi, Y., Chen, K., Zhu, L., Fan, S. (2017). A Comprehensive Photonic Approach for Solar Cell Cooling. ACS Photonics, 4(4), 774-782. https://doi.org/10.1021/acsphotonics.7b00089

[16] Perrakis, G., Tasolamprou, A.C., Kenanakis, G., Economou, E.N., Tzortzakis, S., Kafesaki, M. (2020). Passive radiative cooling and other photonic approaches for the temperature control of photovoltaics: A comparative study for crystalline silicon-based architectures. Optics Express, 28(13): 18548. https://doi.org/10.1364/oe.388208

[17] Lu, K., Zhao, B., Xu, C., Li, X., Pei, G. (2022). A full-spectrum synergetic management strategy for passive cooling of solar cells. Solar Energy Materials and Solar Cells, 245: 111860. https://doi.org/10.1016/j.solmat.2022.111860

[18] Suryanto, S., Firman, F. (2016). The vacuum technique for cooling PV cell. In Proceedings of the First Mandalika International Multi-Conference on Science and Engineering 2022, MIMSE 2022 (Mechanical and Electrical) (MIMSE-M-E-I-2022). https://doi.org/10.2991/978-94-6463-078-7_13

[19] Ahmadi Moghaddam, H., Tkachenko, S., Yeoh, G.H., Timchenko, V. (2023). A newly designed BIPV system with enhanced passive cooling and ventilation. Building Simulation, 16(11): 2093-2107. https://doi.org/10.1007/s12273-023-1051-z

[20] Zhao, B., Hu, M., Ao, X., Xuan, Q., Pei, G. (2020). Spectrally selective approaches for passive cooling of solar cells: A review. Applied Energy, 262: 114548. https://doi.org/10.1016/j.apenergy.2020.114548

[21] Dubey, S., Sarvaiya, J.N., Seshadri, B. (2013). Temperature dependent photovoltaic (PV) efficiency and its effect on PV production in the world – A review. Energy Procedia, 33: 311-321. https://doi.org/10.1016/j.egypro.2013.05.072

[22] Agyekum, E.B., Praveenkumar, S., Alwan, N.T., Velkin, V.I., Shcheklein, S.E., Yaqoob, S.J. (2021). Experimental investigation of the effect of a combination of active and passive cooling mechanism on the thermal characteristics and efficiency of solar PV module. Inventions, 6(4): 63. https://doi.org/10.3390/inventions6040063

[23] Duan, J. (2021). A novel heat sink for cooling concentrator photovoltaic system using PCM-porous system. Applied Thermal Engineering, 186: 116522. https://doi.org/10.1016/j.applthermaleng.2020.116522

[24] Vijaya, G., Muralidhar Singh, M., Krupashankara, M.S., Kulkarni, R. (2016). Effect of argon gas flow rate on the optical and mechanical properties of sputtered tungsten thin film coatings. IOP Conference Series: Materials Science and Engineering, 149(1): 012075. https://doi.org/10.1088/1757-899X/149/1/012075

[25] Tadepalli, S.C., Erdemir, A., Cavanagh, P.R. (2011).

Comparison of hexahedral and tetrahedral elements in finite element analysis of the foot and footwear. Journal of Biomechanics, 44(12): 2337-2343. https://doi.org/10.1016/j.jbiomech.2011.05.006

[26] Shen, C., Zhang, Y., Zhang, C., Pu, J., Wei, S., Dong, Y. (2021). A numerical investigation on optimization of PV/T systems with the field synergy theory. Applied Thermal Engineering, 185: 116381. https://doi.org/10.1016/j.applthermaleng.2020.116381

[27] Smets, A., Jäger, K., Isabella, O., Van Swaaij, R., Zeman, M. (2016). Solar Energy: The physics and engineering of photovoltaic conversion, technologies and systems. Bloomsbury Publishing.

[28] Sab, A., Vogl, U., Weitz, M. (2011). Laser cooling of a potassium-argon gas mixture using collisional redistribution of radiation. Applied Physics, 102(3): 503-507. https://doi.org/10.1007/s00340-011-4401-y

[29] Jaffar, M.F., Mohammad, A.T., Ahmed, A.Q. (2022). An experimental study for enhancing the performance of the photovoltaic module using forced air. Journal of Techniques, 4(2): 1–9. https://doi.org/10.51173/jt.v4i2.462

[30] Liu, P., Justo Alonso, M., Mathisen, H.M., Halfvardsson, A. (2022). The use of machine learning to determine moisture recovery in a heat wheel and its impact on indoor moisture. Building and Environment, 215: 108971. https://doi.org/10.1016/j.buildenv.2022.108971

[31] Cuce, E. (2018). Accurate and reliable U-value assessment of argon-filled double glazed windows: A numerical and experimental investigation. Energy and Buildings, 171: 100-106. https://doi.org/10.1016/j.enbuild.2018.04.036

[32] Sismanoglu, B.N., Maciel, H.S., Marija Radmilovic-Radjenovic, R.S.P. (2013). Argon Production, Characteristics And Applications. NOVA Publishers, NY: USA.

[33] Shukla, A., Kant, K., Sharma, A., Biwole, P.H. (2017). Cooling methodologies of photovoltaic module for enhancing electrical efficiency: A review. Solar Energy Materials and Solar Cells, 160: 275-286. https://doi.org/10.1016/j.solmat.2016.10.047

[34] Sato, D., Yamada, N. Review of photovoltaic module cooling methods and performance evaluation of the radiative cooling method Renew. Renewable and Sustainable Energy Reviews 104: 151-166. https://doi.org/10.1016/j.rser.2018.12.051

[35] Zhao, B., Hu, M., Ao, X., Pei, G. Performance analysis of enhanced radiative cooling of solar cells based on a commercial silicon photovoltaic module. Solar Energy 176: 248-255. https://doi.org/10.1016/j.solener.2018.10.043

[36] Dwivedi, P., Sudhakar, K., Soni, A., Solomin, E., Kirpichnikova, I. (2020). Advanced cooling techniques of PV modules: A state of art. Case Studies in Thermal Engineering, 21: 100674. https://doi.org/10.1016/j.csite.2020.100674

[37] Al-Waeli, A.H.A., Kazem, H.A., Chaichan, M.T., Sopian, K. (2019). Photovoltaic/thermal (PV/T) systems: principles, design, and applications. Springer Nature. https://doi.org/10.1007/978-3-030-27824-3

[38] H.G. Teo, P.S. Lee, M.N. Hawlader. An active cooling system for photovoltaic modules. Applied Energy, 90(1): 309-315. https://doi.org/10.1016/j.apenergy.2011.01.017

[39] S. Wu, C. Xiong. Passive cooling technology for photovoltaic panels for domestic houses. International Journal of Low-Carbon Technologies, 9(2): 118-126. https://doi.org/10.1093/ijlct/ctu013

[40] Sharma, R., Singh, S., Mehra, K.S., Kumar, R. Performance enhancement of solar photovoltaic system using different cooling techniques. Materials Today Proceedings, 46(20): 11023-11028. https://doi.org/10.1016/j.matpr.2021.02.132